Thickness and Closure Kinetics of the Suprachoroidal Space Following Microneedle Injection of Liquid Formulations

Bryce Chiang,[1] Nitin Venugopal,[2] Hans E. Grossniklaus,[3] Jae Hwan Jung,[4] Henry F. Edelhauser,*[,3] and Mark R. Prausnitz[1,4]

[1]Wallace H. Coulter Department of Biomedical Engineering at Georgia Tech and Emory University, Georgia Institute of Technology, Atlanta, Georgia, United States
[2]H. Milton Stewart School of Industrial & Systems Engineering, Georgia Institute of Technology, Atlanta, Georgia, United States
[3]Emory Eye Center, Emory University, Atlanta, Georgia, United States
[4]School of Chemical & Biomolecular Engineering, Georgia Institute of Technology, Atlanta, Georgia, United States

Correspondence: Mark R. Prausnitz, School of Chemical and Biomolecular Engineering, Georgia Institute of Technology, 311 Ferst Drive, Atlanta, GA 30332, USA; prausnitz@gatech.edu.

*Deceased December 5, 2015

Submitted: July 23, 2016
Accepted: November 21, 2016

Citation: Chiang B, Venugopal N, Grossniklaus HE, Jung JH, Edelhauser HF, Prausnitz MR. Thickness and closure kinetics of the suprachoroidal space following microneedle injection of liquid formulations. *Invest Ophthalmol Vis Sci*. 2017;58:555–564. DOI:10.1167/iovs.16-20377

Purpose. To determine the effect of injection volume and formulation of a microneedle injection into the suprachoroidal space (SCS) on SCS thickness and closure kinetics.

Methods. Microneedle injections containing 25 to 150 μL Hanks' balanced salt solution (HBSS) were performed in the rabbit SCS ex vivo. Distribution of SCS thickness was measured by ultrasonography and three-dimensional (3D) cryo-reconstruction. Microneedle injections were performed in the rabbit SCS in vivo using HBSS, Discovisc, and 1% to 5% carboxymethyl cellulose (CMC) in HBSS. Ultrasonography was used to track SCS thickness over time.

Results. Increasing HBSS injection volume increased the area of expanded SCS, but did not increase SCS thickness ex vivo. With SCS injections in vivo, the SCS initially expanded to thicknesses of 0.43 ± 0.06 mm with HBSS, 1.5 ± 0.4 mm with Discovisc, and 0.69 to 2.1 mm with 1% to 5% CMC. After injection with HBSS, Discovisc, and 1% CMC solution, the SCS collapsed to baseline with time constants of 19 minutes, 6 hours, and 2.4 days, respectively. In contrast, injections with 3% to 5% CMC solution resulted in SCS expansion to 2.3 to 2.8 mm over the course of 2.8 to 9.1 hours, after which the SCS collapsed to baseline with time constants of 4.5 to 9.2 days.

Conclusions. With low-viscosity formulations, SCS expands to a thickness that remains roughly constant, independent of the volume of fluid injected. Increasing injection fluid viscosity significantly increased SCS thickness. Expansion of the SCS is hypothesized to be controlled by a balance between the viscous forces of the liquid formulation and the resistive biomechanical forces of the tissue.

Keywords: suprachoroidal space, suprachoroidal space thickness, microneedle injection, ocular drug delivery, 3D cryo-reconstruction

The suprachoroidal space (SCS) is a potential space found between the sclera and choroid. Due to its close proximity to the ciliary body, choroid, retina, and sclera, this space has recently drawn attention as a site for targeted drug delivery,[1–7] placement of glaucoma drainage devices,[8–11] and implantation of retinal prostheses.[12] As a site of drug administration, delivery into the SCS is noted for high bioavailability at targeted tissues in posterior segment diseases, as well as fast clearance by the choroidal vasculature.[3,13] Access to the SCS is possible via surgical procedures of varying complexity[6,7,14–18] and using microneedle injections that offer greater simplicity.[3,5] A hollow microneedle with a length similar to the thickness of the sclera can be used to reliably access the SCS while preventing penetration deeper into the eye.[3,5] Microneedle injections can be performed by ophthalmologists in the outpatient clinic setting, similar to the intravitreal injection procedure. The safety and efficacy of these microneedle injections were demonstrated in a recent open-label Phase I/II clinical trial (NCT01789320 and NCT02255032), and a Phase III clinical trial is ongoing (NCT02595398) to further study the efficacy of drug delivery to the SCS.

Although many studies have investigated the two-dimensional (2D) circumferential spread of particles[1,3,5,19–22] and molecules[4,13,20,23,24] within the SCS, few have studied the third dimension: the distensibility of the choroid off the sclera, also known as the SCS thickness. Seiler et al.[24] measured the maximum SCS thickness over the injection site in ex vivo porcine and canine eyes, and found that there was no difference in thickness with three injection volumes, especially once the eyes were inflated to a physiological intraocular pressure. They also determined the three-dimensional (3D) distribution of microbubbles in the porcine eye.[24] However, microbubbles are not expected to distribute in the same way as neutral-density materials.[21] Patel et al.[3,5] used a fluorophotometer to assess the SCS thickness along the visual axis in rabbits. Gu et al.[20] used optical coherence tomography to study the SCS thickness along the visual axis in guinea pigs. Since the injection occurs in the far periphery (near the limbus), the SCS

Investigative Ophthalmology & Visual Science

thickness at the posterior pole may not be representative of the entire globe. Kadam et al.[25] showed that the physiochemical properties of molecules injected into the SCS affected affinity to certain ocular layers, which may indirectly affect measured SCS thickness.

The purpose of this study was to evaluate the effect of injection volume and liquid formulation viscosity on SCS thickness at the time of injection and over time after the injection. We used two companion approaches to report on the distribution of the SCS thickness throughout the entire ocular globe (i.e., ultrasonography and 3D cryo-reconstruction).

We hypothesize that for a given liquid formulation, the SCS thickness expands to a constant value independent of the volume of fluid injected; that increasing viscosity of the liquid formulation increases the SCS thickness; that SCS thickness may continue to expand after injection of concentrated carboxymethyl cellulose (CMC) solutions forming physically crosslinked hydrogels that swell; and that SCS thickness collapses to baseline over time after SCS injection.

Materials and Methods

All reagents and chemicals were purchased from Sigma-Aldrich Corp. (St. Louis, MO, USA) unless otherwise specified. Red-fluorescent polystyrene particles (excitation: 580 nm; emission: 605 nm) with diameters of 200 nm were purchased from Life Technologies (Fluospheres; Carlsbad, CA, USA). Eyes of pigmented Silver Fox and American Blue rabbits (Broad River Pastures, Elberton, GA, USA) and albino New Zealand White rabbits (Pel-Freez, Rogers, AR, USA) were obtained within 1 day after euthanasia and stored in a −80°C freezer immediately upon arrival. Pigmented eyes were used to prevent vitreous glow (Supplementary Fig. S3). There was no gross anatomic difference among the eyes beyond eye size. All in vivo experiments were carried out in albino New Zealand White rabbits (Charles River Laboratories, Wilmington, MA, USA) and were approved by the Georgia Institute of Technology Institutional Animal Care and Use Committee. Practices complied with the ARVO Statement for the Use of Animals in Ophthalmic and Vision Research. Four replicates per group were performed unless otherwise specified.

Ex Vivo Injection Procedure

Using a rabbit eye pressurized to physiological intraocular pressure (IOP), a 750-μm-long, 33-gauge hollow microneedle attached to a syringe was used to make injections of red-fluorescent particles suspended in 25 to 150 μL Hanks' balanced salt solution (HBSS) into the SCS. See Supplementary Information (SI) for details.

Effect of Injection Volume on SCS Thickness

To perform 3D cryo-reconstruction imaging, microneedle injections of 25 to 150 μL containing red-fluorescent particles were performed in pigmented rabbit eyes, which were frozen 3 minutes post injection and prepared for cryosectioning. Using a digital camera, one red-fluorescent image of the cryoblock of tissue was obtained every 300 μm by slicing the sample with the cryostat. Image stacks consisting of red-fluorescence images were analyzed to determine SCS thickness. See SI for details.

Ultrasound B-Scan Method

A high-frequency ultrasound (U/S) probe (UBM Plus; Accutome, Malvern, PA, USA) was used to determine SCS thickness by generating 2D cross-sectional images of the SCS in rabbit eyes ex vivo after injecting volumes ranging from 25 to 150 μL. Three minutes after injection, the U/S probe was used to acquire eight sagittal views around the eye. Postprocessing of the U/S B-scans was performed to find the thickness from the outer sclera to the inner retina at 1, 5, and 9 mm posterior to the scleral spur. See SI for details.

Mechanical Testing of Sclera–Choroid Attachments

After microneedle injection of 100 μL HBSS into the SCS of albino rabbit eyes ex vivo, two sagittal strips—one with no injection and one with SCS injection—from the same eye were each mounted on a force displacement station that peeled the sclera from the choroid to determine the average force to separate the tissues. See SI for details.

Effect of Liquid Formulation on SCS Thickness and Collapse Time

After injection of a formulation into the SCS of an anesthetized rabbit, U/S B-scan was used to determine SCS thickness at multiple locations over time, from which the rate of SCS collapse was calculated. See SI for details. In companion experiments, the approximate clearance rate of injected fluorescent material from the SCS was found by taking fluorescence fundus images in the rabbit eye in vivo over time until fluorescence was no longer visible. See SI for details.

Results

Effect of Injection Volume on SCS Thickness

We measured the thickness of the SCS and investigated its distribution in rabbit eyes after microneedle injection ex vivo using a 3D cryo-reconstruction method. Two-dimensional mapping of the spread of particles (Fig. 1A) in the SCS after injection of different volumes of fluid indicated that the area of spreading increased with injection volume.

Quantification of the SCS thickness throughout the area of spreading produced histograms (Fig. 1B) of the SCS thickness for each injection volume. Sites where SCS thickness was less than 25 μm were considered to have "unopened" SCS and were therefore not included in the analysis. All particle thickness histograms showed a characteristic spike at ∼160 μm (i.e., the average mode value among the histograms collected at all conditions shown in Fig. 1 is 160 ± 25 μm [mean ± SEM]), and there were very few portions of the SCS open to smaller thicknesses. This peak value of SCS thickness did not significantly change as a function of injection volume ($P = 0.43$, 1-way ANOVA). This indicates that if the SCS is opened up, it readily expands to a thickness of at least ∼160 μm.

The median value of SCS thickness was found to be 330 ± 30 μm, which was significantly different from the mode value ($P < 0.001$, unpaired t-test) indicating few points where the thickness was less than 150 μm. The median SCS thickness was independent of injection volume ($P = 0.15$, F-test for zero slope), as shown in Figure 1C. This finding is notable, because injection of larger volumes of fluid can increase the area of fluid spread in the SCS and/or the thickness of the SCS. These data indicate that the SCS expands to a maximum thickness, and that injection of additional fluid increases area of spreading in direct proportion to the volume injected. To further test this hypothesis, we plotted area of spreading versus injection volume and found that they increased in direct proportion to each other (Supplementary Fig. S4).

Investigative Ophthalmology & Visual Science

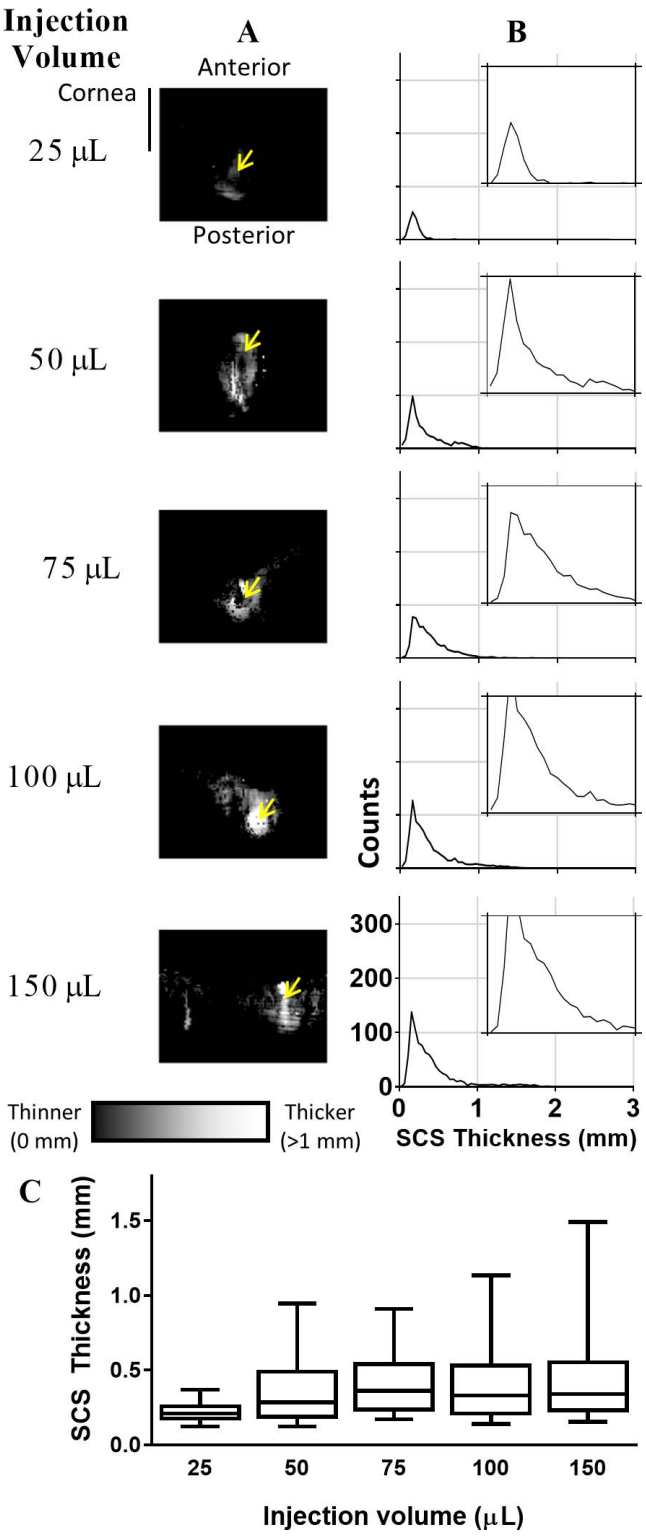

FIGURE 1. Distribution of SCS thickness after injection of particles suspended in HBSS into the SCS of the rabbit eye ex vivo. Rabbit eyes were frozen 1 minute after SCS injection and analyzed by 3D cryo-reconstruction. (**A**) Representative thickness maps of 200-nm particles, where *brighter white color* indicates thicker SCS spreading. *Yellow arrow* indicates site of injection, at the 12 o'clock superior position. Each 2D map is an equatorial projection oriented such that anterior (i.e., cornea) is up and posterior (i.e., optic nerve) is down. As with 2D map projections of globes, the areas represented by pixels at the upper and lower poles are distorted. (**B**) Data from these thickness maps are presented as histograms for different injection volumes (indicated on the *right side* of the figure). The *y*-axis is counts with every 100 counts marked. (**C**) Box and whiskers represent 5th, 25th, 50th (median), 75th, and 95th percentile of SCS thickness after injection (n = 3–7 replicates per condition).

Finally, the mean values of SCS thickness were found to be 340 ± 40 μm among all the conditions tested. The mean values had a slight dependence on injection volume ($P = 0.04$, F-test for zero slope). The 5th, 25th, median, and 75th percentile SCS thickness was approximately constant for injection volumes greater than 25 μL, but the 95th percentile increased with injection volume. The fact that there was a spread of SCS thicknesses to values up to a few-fold larger than the median value indicates that SCS thickness can be spread well beyond ~300 μm in some cases. These sites of greater SCS thickness occurred in patches (see bright spots on Fig. 1A) that were often located near the site of injection.

Ultrasound B-Scan Measurement

To validate the SCS thickness measurements calculated by the cryo-reconstruction method, we conducted additional experiments to measure SCS thickness by ultrasound B-scan in the rabbit eye ex vivo (Fig. 2). This U/S measurement yielded a median SCS thickness of 160 ± 20 μm, which was independent of injection volume ($P = 0.67$, F-test for zero slope) and was approximately half the value obtained by the cryo-reconstruction method (i.e., 330 ± 30 μm). However, the two methods both showed that SCS thickness values were independent of injection volume and had a median value between 150 and 350 μm. Since the eyes used in the U/S measurement were at room temperature and measured in real time shortly after injection, whereas the eyes used in 3D cryo-reconstruction were frozen shortly after injection and measured later while still in the frozen state, the observed differences in thickness may be due to differences in timing, temperature, solid versus liquid state tissue fluids, or artifacts due to freezing. Furthermore, the U/S measurement was not able to assess the SCS thickness at the posterior pole, which may have biased the results.

Measurement of Force of Adhesion Between Sclera and Choroid

We investigated further why median SCS thickness was constant over the range of injection volumes studied. The presence of lamellae that attach the sclera to the choroid might explain this constant thickness, as they may limit expansion of the SCS beyond a certain thickness.[16,26,27] We therefore performed a peel test (Fig. 3A) on scleral/chorioretinal strips from rabbit eyes that had either received or not received a SCS injection of HBSS ex vivo. We found that eyes with previous injection in the SCS required only 51% of the force to separate the sclera from the choroid compared with eyes having no SCS injection ($P < 0.005$, unpaired t-test, Fig. 3B). This suggests that the process of SCS injection weakens the adhesion strength between the sclera and choroid, possibly due to reorganizing, weakening, breaking, or otherwise altering fibers adhering the sclera to the choroid. Since the force to separate the tissue does not become zero after injection, adhesive forces between the sclera and choroid, possibly involving connective fibers, may play a role in limiting SCS expansion.

To further interpret these findings, we examined histologic sections for anatomic structures within the SCS of rabbit eyes that had either received or not received a SCS injection of HBSS

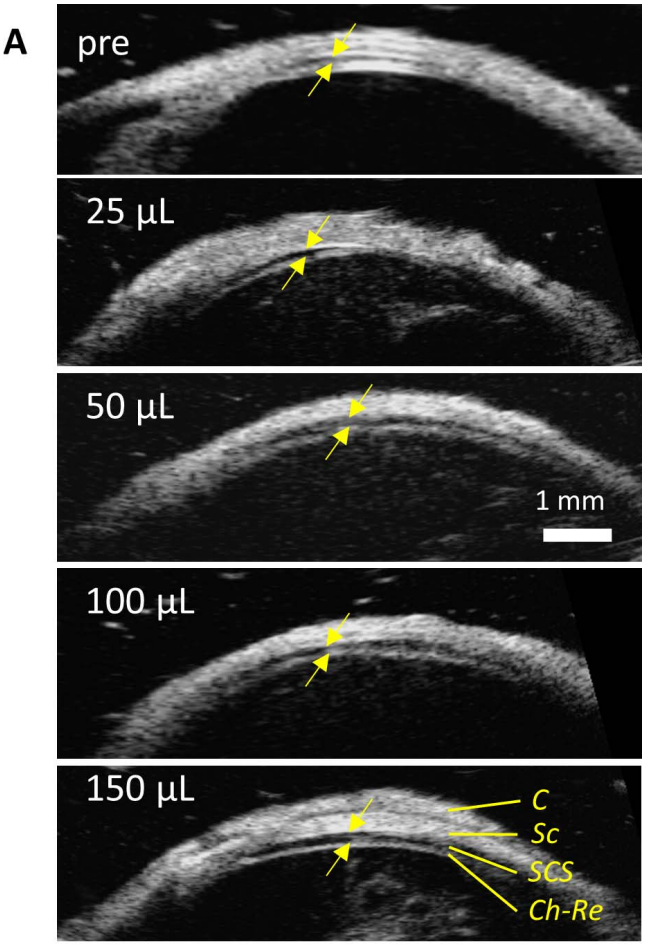

FIGURE 2. SCS thickness measured with ultrasound B-scan in the rabbit eye ex vivo. (**A**) Representative ultrasound B-scans. (**B**) Quantification of median SCS thickness ± SEM based on ultrasound (U/S) and cryo-reconstruction methods ($n = 3$–7 replicates). *Lines* on the graph indicate best fits by linear regression. C, conjunctiva; Sc, sclera; SCS, suprachoroidal space; Ch-Re, choroid-retina. *Arrows* indicate SCS thickness.

in the live rabbit. With no injection, the sclera and choroid were tightly apposed (Fig. 4A). After injection, the sclera and choroid were no longer tightly adhered (Fig. 4B), even more than 1 month after injection in vivo (Fig. 4C). Furthermore, there was evidence of structures that appear to be fibrils

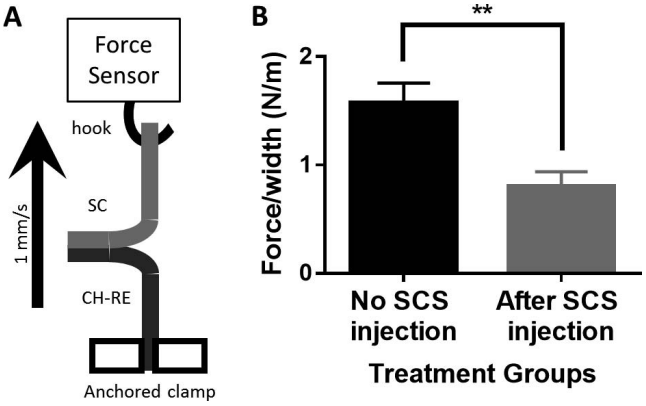

FIGURE 3. Modified ATSM 1876 peel test performed on scleral/chorioretinal (Sc-Ch-Re) strips from eyes that either had received (*gray bar*) or not received (*black bar*) a 100-µL SCS injection of HBSS ex vivo. (**A**) A diagram of the experimental setup is shown. (**B**) Mean ± SEM of the force to separate sclera from choroid per width of tissue strip is shown ($n = 8$ replicates). $P < 0.005 = **$, unpaired *t*-test.

connecting the sclera and choroid (Figs. 4B, 4C). It cannot be determined at this time if these fibrils were intact or not. In companion experiments, the SCS thickness measured in vivo by U/S 30 minutes or longer post injection was found to be indistinguishable from preinjection thickness (i.e., zero), suggesting that processes in the living rabbit (e.g., intraocular pressure) were able to minimize the SCS thickness in vivo but were unable to maintain it after death. This finding further supports the hypothesis that there has been a loss in adhesion strength, possibly due to changes to the SCS lamellae.

Effect of Liquid Formulation on SCS Thickness and Collapse Time

We next evaluated the effect of liquid formulation on SCS thickness, as well as the SCS collapse rate over time in the living rabbit (Fig. 5A). We chose solutions of CMC at different concentrations in HBSS and the commercial viscoelastic product Discovisc (Alcon, Fort Worth, TX, USA) (which contains 1.65 MDa hyaluronic acid) as liquid formulations for this study, because these liquid formulations were previously shown to distribute differently in the SCS, compared with HBSS.[19]

The initial SCS thickness at the injection site varied greatly with choice of liquid formulation from 0.43 ± 0.06 mm with HBSS to 2.1 ± 0.1 mm with 5% CMC in HBSS (Figs. 5B, 6). The value for HBSS found here in the living rabbit eye is larger than what was found as explained above in the rabbit eye ex vivo. This could be because the in vivo measurement was made at the injection site, which was the site of maximum SCS thickness, whereas the ex vivo measurement was reported as the average SCS thickness through the expanded SCS. Use of Discovisc, which had previously been reported to initially remain near the site of injection in the SCS,[19] showed a SCS thickness of 1.5 ± 0.4 mm, which was significantly larger than the value for HBSS ($P < 0.01$, Sidak's multiple comparison test). Suprachoroidal space injection of solutions containing 1%, 3%, and 5% CMC in HBSS (viscous solutions that have also been reported to localize at the injection site[19]) had initial SCS thicknesses of 0.7 ± 0.1, 1.6 ± 0.2, and 2.1 ± 0.1 mm, respectively (Fig. 5B). These data indicate that changing the formulation (to increase viscosity) had a larger effect on SCS thickness than increasing injection volume for a given formulation.

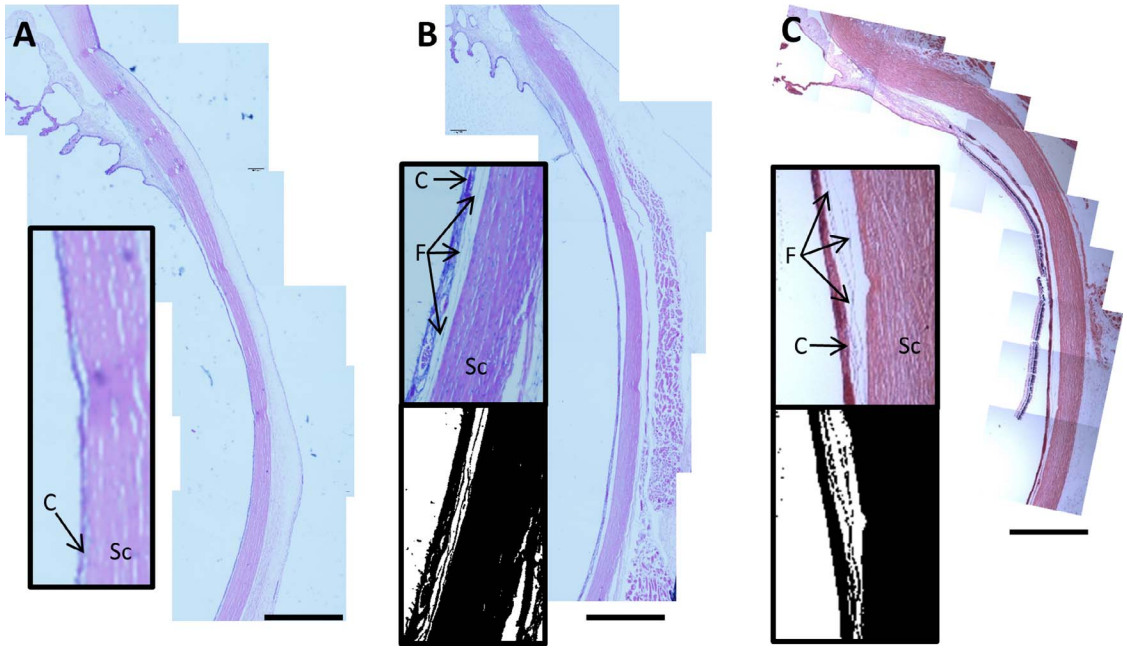

FIGURE 4. Representative histologic images showing evidence of SCS fibrils. (**A**) In eyes with no injection, the sclera and choroid were tightly adhered. (**B**) In eyes 30 minutes after HBSS injection, the sclera and choroid were no longer closely adherent. There are SCS fibrils visible, especially when the image is transformed to *black and white* (*insets*). (**C**) In eyes 1+ month after HBSS injection, the sclera and choroid were still not adherent, and there are SCS fibrils visible. When animals were viewed using U/S in vivo, no SCS expansion was visible (data not shown). Sc, sclera; C, choroid; F, SCS fibril. *Scale bar*: 1 mm.

We next monitored SCS thickness over time at eight positions around the globe for all the formulations tested (Supplementary Fig. S5). After injection of HBSS, the SCS thickness over the injection site achieved its peak value immediately after injection and then decreased according to a roughly first-order exponential decay; that is, there was no significant difference between SCS thickness immediately post injection (θ_0) and the maximal SCS thickness (θ_{max}) ($P > 0.99$, Sidak's multiple comparison test, Fig. 5B). Measurements at other locations around the globe behaved similarly.

There was also no difference between initial and maximal SCS thickness over the injection site for Discovisc and 1% CMC ($P \geq 0.97$, Sidak's multiple comparison test). However, the SCS thickness measured at the other sites behaved differently, which is consistent with a previous study.[19] With Discovisc, the decrease in SCS thickness at the injection site over time was accompanied by a concomitant increase in SCS thickness at adjacent sites in the SCS (Supplementary Fig. S5A, 4 hours). By 2 days, the SCS thickness throughout the entire eye had returned to baseline. In contrast, 1% CMC expanded the SCS only at or near the injection site for the entire time course (data not shown). Because Kim et al.[19] had shown that Discovisc was able to facilitate the distribution of particles throughout the SCS and that CMC was able to localize particles near the injection site, we hypothesize that the expansion of a region of SCS was necessary for particle deposition in that region.

With 3% CMC and 5% CMC solutions, θ_0 over the injection site was different than θ_{max} ($P < 0.01$, 2-way ANOVA) because the SCS thickness initially increased over the course of hours after the injection. This expansion of the SCS could be explained by an osmotic and hydration effect of the CMC within the SCS, which could draw in water from the surrounding tissue to dilute the CMC and cause swelling of the gel. Besides the swelling at the site of injection, the behavior of the SCS thickness at other positions (Supplementary Fig. S4B) was similar to that found with 1% CMC.

To describe the time course of SCS thickness changes after injection over the injection site, we used a second-order exponential equation that could account for both the observed expansion and collapse of the SCS:

$$\theta(t) = -Ae^{-t/\tau_{exp}} + Be^{-t/\tau_{col}}, \quad (1)$$

where t is the time post injection, $\theta(t)$ is the SCS thickness as a function of time, A and B are thickness constants, τ_{exp} is the expansion time constant, and τ_{col} is the collapse time constant (Fig. 5C). This equation described the data from all the liquid formulations well (Pearson coefficient $r^2 > 0.76$).

Using this equation, we calculated the characteristic times associated with each of the liquid formulations. As expected, the liquid formulations that did not cause further expansion of the SCS after injection (i.e., HBSS, Discovisc, and 1% CMC) had calculated τ_{exp} values were all on the order of seconds (Fig. 5C, left). In contrast, τ_{exp} values for the 3% CMC and 5% CMC liquid formulations ranged from 2.8 to 9.1 hours, and there was no significant difference among these τ_{exp} values ($P = 0.77$, F-test).

There were significant differences in τ_{col} values among the liquid formulations tested (Fig. 5C, right). With HBSS as the liquid formulation, τ_{col} was 19 ± 3 minutes. With the Discovisc liquid formulation, τ_{col} was 6 ± 2 hours, which was significantly longer than the HBSS value ($P < 0.005$, F-test). With all of the CMC liquid formulations, τ_{col} ranged from 2.4 to 9.2 days, which was also longer than for HBSS ($P < 0.0001$, F-test) but not different with respect to each other ($P = 0.47$, F-test). It is notable that collapse of SCS-containing 1% CMC solution (that did not swell after injection) and SCS-containing 5% CMC solution (which did swell after injection) had comparable τ_{col} values, which suggests that dissociation of the crosslinks found in CMC gels[28] is the rate-limiting step to CMC clearance from the SCS resulting in collapse.

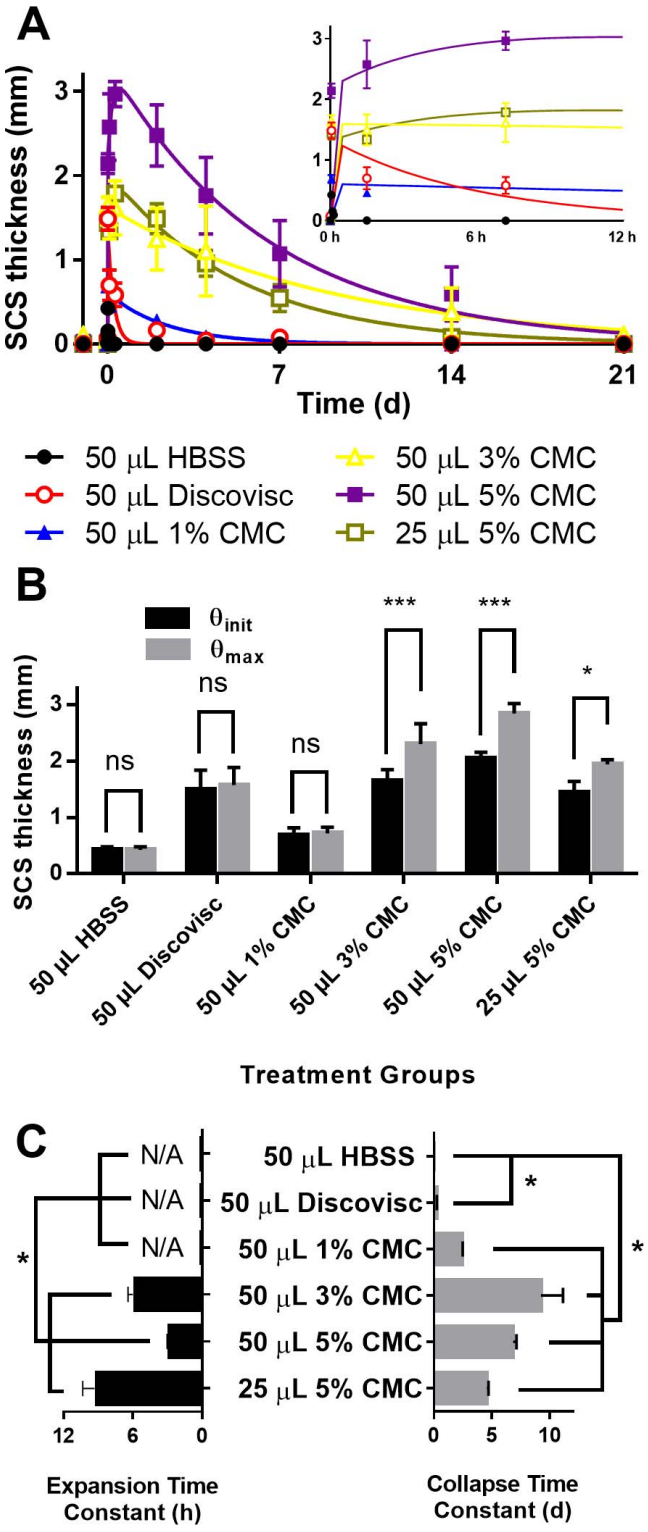

Figure 5. Quantification of median SCS thickness after injection of different liquid formulations as a function of time. (**A**) Time course of SCS thickness after injection with six liquid formulations. *Inset* shows first 24 hours. (**B**) SCS thickness measured immediately post injection (θ_0) and the maximum SCS thickness reached (θ_{max}) when using different liquid formulations. (**C**) The time constants associated with SCS expansion and collapse when using different liquid formulations. All values are mean ± SEM ($n = 4$ replicates) (ns = no significant difference, $P < 0.05$ = *; $P < 0.0005$ = ***, *F*-test).

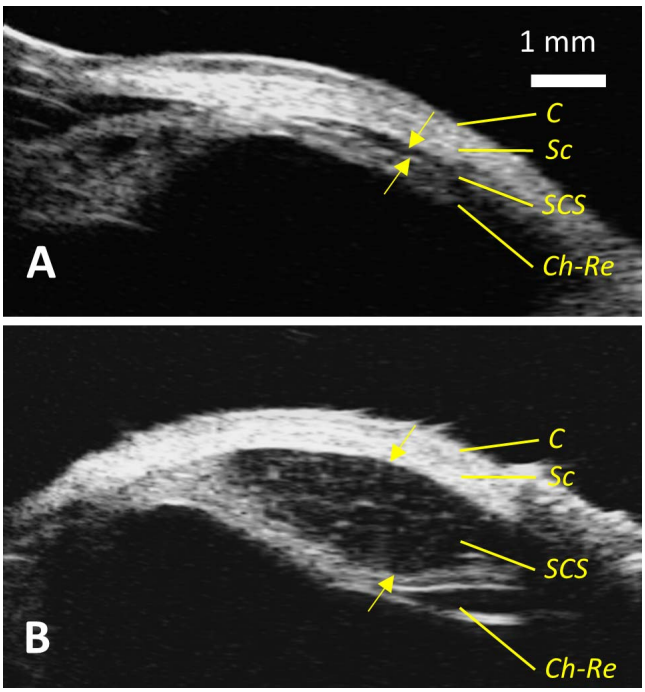

Figure 6. Representative ultrasound B-scan images of the SCS after 50-µL injection of (**A**) HBSS and (**B**) 5% CMC solution. C, conjunctiva; Sc, sclera; SCS, suprachoroidal space; Ch-Re, choroid-retina. *Arrows* indicate SCS thickness.

Effect of Liquid Formulation on Clearance of Fluorescent Molecules From the SCS

We investigated the effect of liquid formulation viscosity on the time scale of clearance of fluorescein from the SCS. Using fundus microscopy, we identified how long it took for there to be no visual evidence of fluorescein in the SCS. Total clearance of fluorescein injected into the SCS in HBSS was 0.33 ± 0.05 days; this was significantly faster than the clearance of fluorescein injected in 5% CMC solution, which was 2.7 ± 0.7 days ($P < 0.0005$, unpaired *t*-test, Fig. 7). This can probably be explained by the long-lived presence of viscous CMC gel in the SCS (as evidenced by the SCS remaining open for many days; Fig. 5; Supplementary Fig. S4), which can slow diffusion of fluorescein out of the SCS.

Discussion

This study examined the effects of injection volume, liquid formulation, and liquid formulation on the thickness and closure kinetics of the SCS following microneedle injection. The effects of other variables, such as injection location,[29] intraocular pressure,[5] molecular physiochemistry,[25] or particle density,[21] have been addressed previously. Since the focus of this study was to explore factors that modulate SCS thickness, the distribution, drainage routes, and kinetics of clearance from the SCS were not addressed here.

Effect of Injection Volume on SCS Thickness

We found that the SCS was spread to a roughly constant thickness, independent of injection volume. The observation was made in the rabbit eye ex vivo using two different measurement methods: 3D cryo-reconstruction and U/S B-scan imaging. This result was not necessarily expected. Injection of an increasing volume of fluid into the SCS could be

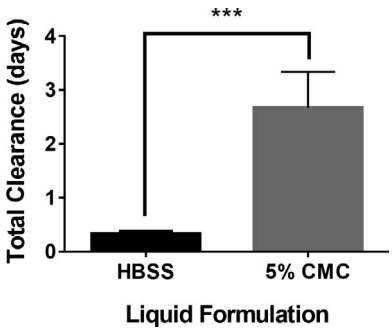

FIGURE 7. The total clearance time of fluorescein from the SCS after injection in HBSS or 5% CMC solution. Total clearance time is defined as the first time point at which fluorescein was not detectable under fluorescence fundus exam. All values are mean ± SEM (n = 3–6 replicates). $P < 0.0005$ = ***, unpaired t-test.

accommodated by an increase in SCS thickness, SCS area, or a combination of both. Our data indicate that the SCS readily expands to a certain thickness, after which additional fluid fills the SCS by expanding the SCS area containing fluid without expanding the SCS thickness further. This explanation was supported by demonstration that the area of fluid in the SCS increased in direct proportion with the volume injected.

We and others hypothesized that the constant SCS thickness could be due to fibrils running between the sclera and choroid that resist expansion of the thickness of this space.[4,27] Results from a modified peel test to determine the strength of adhesion between sclera and choroid showed that a fluid injection into the SCS as a pretreatment reduced, but did not eliminate, the force needed to subsequently separate the tissues. This could be explained by a partial weakening of the adhesions between sclera and choroid, possibly due to reorganizing, weakening, breaking, or otherwise altering the fibrils with an injection. We also imaged evidence of these fibrils in the SCS, which was consistent with previous reports.[26,27]

Previous studies were inconclusive regarding the relationship between SCS thickness and injection volume. Patel et al.[3] used a fluorophotometer to assess the distribution of fluorescein along the visual axis and was able to demonstrate localization in the SCS. No comment was made on the SCS thickness.

Seiler et al.[24] concluded that, in ex vivo canine and porcine eyes, there was a difference between the maximum thickness achieved with the smallest injection volume tested (250 μL) and higher injection volumes tested (500, 800, and 1000 μL). However, no difference in maximum thickness was seen once the eyes were inflated to physiological intraocular pressures.[24] Moreover, the Seiler study assessed maximum thickness, rather than median thickness reported here, and it used much larger volumes of fluid, which are much greater than those used in current clinical trials (Goldstein DA, et al. *IOVS* 2015;56:ARVO E-Abstract 3557).

Gu et al.[20] found that, in guinea pigs, the cross-sectional area of the SCS increased with increasing injection volume. However, as seen in Figure 2A of this study, not all the SCS was expanded, especially at small injection volumes. Thus, increases in cross-sectional area could be attributed to either expanding previously unexpanded SCS (i.e., to enlarge the area of SCS expansion) or increases in SCS thickness.

Effect of Liquid Formulation on SCS Thickness and Collapse Time

We found that liquid formulation had a major effect on SCS thickness, possibly related to fluid viscosity. While HBSS spread over large areas of the SCS, Discovisc and CMC solutions were largely retained near the site of injection initially, probably due to their high viscosity. This might be explained by the viscous forces resisting spread of the injected fluid in the SCS leading to the fluid further expanding the SCS near the site of injection in order to accommodate the injected fluid volume. Interestingly, in some cases (i.e., 3% CMC and 5% CMC solutions), SCS thickness continued to expand for hours after the injection, probably due to the diffusion of water into the hydrogel, which resulted in swelling it.

At later times, SCS thickness decreased and ultimately returned to baseline within hours for HBSS and within days to weeks for the viscous solutions. Clearance kinetics and routes were described in another study.[30] These slow kinetics were probably controlled by clearance of the polymer components of the hydrogels from the SCS, which was significantly slower for CMC, which forms a physically crosslinked gel.[28]

Other formulations,[1,7,15,21,24,31–36] including in situ gelling formulations (such as poly[ortho esters][7] or polycaprolactone dimethacrylate[15]), have been injected into the SCS, but those studies did not report on SCS thickness or closure times. These formulations may exhibit behavior, at least initially, that is qualitatively similar to that seen with CMC or Discovisc in this study, depending in part on formulation viscosity. Our formulations also contained particles, which are not expected to change the clearance properties of the polymeric formulation.[20,37]

We propose that SCS thickness is controlled by a balance between the viscous forces of the liquid formulation and the biomechanical forces inherent to the tissue (such as the viscoelastic properties of the sclera and choroid, as well as the viscoelastic and failure mechanics of the SCS fibrils). A cartoon of this is presented in Figure 8. When fluid first enters the SCS, it can expand the thickness of the SCS at the site of injection, and/or it can expand the area of the SCS that it occupies. We propose that what determines how the SCS expands to accommodate the fluid is based on whether there is less physical resistance to increasing thickness or to increasing area. Increasing thickness requires overcoming biomechanical forces (e.g., from fibrils connecting sclera to choroid), elastic restoring forces of the sclera and choroid tissues,[38–40] and intraocular pressure.[41] Increasing area requires overcoming the viscous forces opposing flow of fluid circumferentially in the SCS.

We hypothesize that when the SCS is fully collapsed, the force required to expand the thickness of the SCS is less than the force to flow liquid through the adjacent collapsed SCS to expand the area. As more fluid is forced into the SCS, the SCS thickness continues to expand until the force required for further expansion of thickness of SCS exceeds the force required to flow fluid out into adjacent SCS. This switch occurs due to two factors: (1) As the SCS thickness increases, the force required to further increase thickness escalates; and (2) as the SCS thickness increases, the viscous forces to flow into adjacent SCS decrease because flow through wider channels exhibits less resistance to flow.

When injecting HBSS (with a low viscosity comparable to water) into SCS of the rabbit, the force balance switches when the SCS is expanded to 150 to 350 μm in the rabbit eye ex vivo and to 400 to 500 μm in the rabbit eye in vivo; we can call this thickness the "equilibrium thickness," because it represents the thickness when the force needed to expand thickness equals the forces needed to expand area of the SCS. In this way, SCS readily expands to the equilibrium thickness until further increasing SCS thickness requires more force than increasing SCS area. A distribution of equilibrium thicknesses is expected, as seen in Figure 8, due to variation in the mechanical properties of the SCS.

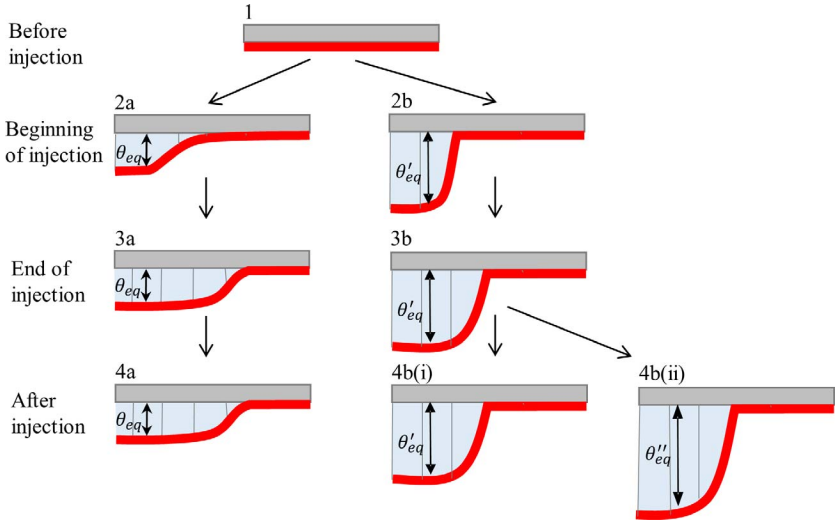

Figure 8. Schematic of SCS expansion after injection of fluid. (**1**) The SCS is closed before injection. (**2**) Upon injection, the SCS expands to an equilibrium thickness (θ_{eq}) determined by a balance between viscous forces of the liquid formulation and the resistive biomechanical forces of the tissue. This thickness is smaller for low-viscosity fluids (θ_{eq} in [**2a**]) than for high-viscosity fluids (θ_{eq}' in [**2b**]), due to increased resistance to flow. (**3**) As the injection proceeds, the area of expanded SCS increases to accommodate the additional fluid, but the SCS thickness remains constant. (**4**) After injection is complete, no further growth of the SCS usually occurs (**4a**, **4b[i]**), but a gel that continues to swell could further increase SCS thickness (θ_{eq}" in [**4b(ii)**]).

When injecting Discovisc or CMC, which have higher viscosity than HBSS (e.g., >170,000 cP for 1.7% CMC [700 kDa] in HBSS[19,28]), the force balance should be altered. The viscous forces of the formulation are increased while the resistive biomechanical forces of the tissue are unchanged. Thus, the equilibrium thickness increases and expansion of SCS area requires greater force.

In the case of 3% CMC and 5% CMC solutions, there is an additional force at play. After the fluid has been injected and the SCS expanded to its equilibrium value, diffusive forces pulling fluid into the CMC gel formed in the SCS cause the gel to expand. Because the gel has physical crosslinks, it cannot easily flow through SCS to expand area, but instead expands in place, which primarily expands SCS thickness. In this case, a new force balance is set up between the expansive swelling force of the gel and the resistive biomechanical forces of the ocular tissue. This results in a new equilibrium thickness based on the balance of these two forces.

Study Limitations

There was a difference between the ex vivo and in vivo SCS thickness. Ex vivo eyes were chosen to remove the confounding effect of fluid clearance from the eye that occurs in vivo. Intraocular pressure changes in postmortem eyes were significantly faster than in eyes in the living rabbit, indicating faster normalization of ocular volume, presumably by clearance of fluid (data not shown). This difference in behavior could be explained by loss of tissue integrity (e.g., loss in the biomechanical strength of sclera or SCS fibrils), the absence of living processes (e.g., choroidal perfusion, intraocular pressure), or consequences of these effects (e.g., increased transscleral and perivascular drainage).

Limitations of the study include use of ex vivo rabbit eyes in some experiments. Species differences between rabbit and human eyes may affect the translation of these findings to clinical medicine. Further experiments in human eyes are warranted. The U/S was able to image only the far periphery, not the posterior aspect of the eye in vivo. This may bias the SCS thickness measurements but should not change the general trends observed.

Conclusions

In conclusion, microneedle injection of fluid into the SCS results in distension of the choroid off the sclera, which expands the thickness of the SCS. Liquid formulation injected into the SCS had a major effect on SCS thickness, where highly viscous fluids expanded SCS thickness more than low-viscosity HBSS. Surprisingly, increasing injection volume of HBSS had little effect on SCS thickness, such that injection of increasing volume of fluid was accommodated by increasing area of fluid spread in the SCS while maintaining constant SCS thickness. Expansion of SCS thickness in vivo ranged from 0.43 ± 0.06 mm after injection of HBSS and 0.7 to 2.8 mm after injection of viscous formulations. Injection of CMC solutions led to further expansion of SCS thickness over the course of hours after the injection was completed, which could be explained by swelling of CMC gel in the SCS. Clearance of HBSS from the SCS occurred within 1 hour and clearance of Discovisc and CMC took days to weeks.

These observations could be explained by SCS expansion controlled by a balance between the viscous forces of the injected liquid formulation (which increase with fluid viscosity) and the biomechanical forces that hold the sclera and choroid together (which are unaffected by fluid viscosity or fluid volume). There is evidence that the forces that limit expansion of SCS thickness may be in part related to fibrils that bind the sclera and choroid and that may need to stretch and/or break to accommodate SCS expansion. These findings that affect the extent and duration of expanded SCS thickness and area may be used to improve control over targeted drug delivery and placement of devices in the SCS for therapeutic applications.

The ability to modulate SCS thickness could have implications on emerging SCS technologies, such as targeted drug delivery, placement of glaucoma drainage devices, and suprachoroidal retinal prostheses. For example, increasing liquid formulation viscosity has a dual effect of expanding the SCS and localizing the circumferential spread at the site of injection. This might be useful in treating localized diseases, such as placing antiglaucoma agents in the anterior SCS near their site of action in the ciliary body[42,43] or localizing anticancer agents in the SCS adjacent to intraocular tumors.

In another application, SCS injections of sodium hyaluronate have been made as an alternative to scleral buckling for the treatment of retinal detachment.[44,45] As shown in the present study, greater distension and localization are achievable with CMC, which continues to expand after injection, compared with hyaluronic acid (i.e., a major component of Discovisc), which does not. Perhaps use of CMC as a liquid formulation may yield better results. Finally, microneedle injection of a viscous liquid formulation could be made prior to surgical implantation of suprachoroidal devices. This could transiently weaken sclera–choroid adhesion (e.g., stretch or break SCS fibrils), allowing for easier implantation.

Acknowledgments

The authors thank Cathy Payne (Broad River Pastures) for graciously providing rabbit eye specimens, Sha'Aqua Asberry for help with histology, Machelle Pardue for use of the RetCam, Victor Breedveld for helpful discussion, and Donna Bondy for administrative support. This work was carried out at the Institute for Bioengineering and Bioscience and Center for Drug Design, Development and Delivery at Georgia Tech.

Supported by National Eye Institute (NEI) Grants EY017045 (BC, HFE, MRP), NEI EY022097 (BC, MRP), NEI EY007092 (BC), NEI EY025154 (BC), and NIH P30EY06360 (HEG).

Disclosure: **B. Chiang**, P; **N. Venugopal**, None; **H.E. Grossniklaus**, None; **J.H. Jung**, None; **H.F. Edelhauser**, Clearside Biomedical (I, C); **M.R. Prausnitz**, Clearside Biomedical (I, C)

References

1. Chen M, Li X, Liu J, Han Y, Cheng L. Safety and pharmacodynamics of suprachoroidal injection of triamcinolone acetonide as a controlled ocular drug release model. *J Control Release*. 2015;203:109–117.
2. Gilger BC, Abarca EM, Salmon JH, Patel S. Treatment of acute posterior uveitis in a porcine model by injection of triamcinolone acetonide into the suprachoroidal space using microneedles. *Invest Ophthalmol Vis Sci*. 2013;54:2483–2492.
3. Patel SR, Berezovsky DE, McCarey BE, Zarnitsyn V, Edelhauser HF, Prausnitz MR. Targeted administration into the suprachoroidal space using a microneedle for drug delivery to the posterior segment of the eye. *Invest Ophthalmol Vis Sci*. 2012;53:4433–4441.
4. Tyagi P, Kadam RS, Kompella UB. Comparison of suprachoroidal drug delivery with subconjunctival and intravitreal routes using noninvasive fluorophotometry. *PLoS One*. 2012;7:e48188.
5. Patel SR, Lin AS, Edelhauser HF, Prausnitz MR. Suprachoroidal drug delivery to the back of the eye using hollow microneedles. *Pharm Res*. 2011;28:166–176.
6. Olsen TW, Feng X, Wabner K, et al. Cannulation of the suprachoroidal space: a novel drug delivery methodology to the posterior segment. *Am J Ophthalmol*. 2006;142:777–787.
7. Einmahl S, Savoldelli M, D'Hermies F, Tabatabay C, Gurny R, Behar-Cohen F. Evaluation of a novel biomaterial in the suprachoroidal space of the rabbit eye. *Invest Ophthalmol Vis Sci*. 2002;43:1533–1539.
8. Garcia-Feijoo J, Rau M, Grisanti S, et al. Supraciliary microstent implantation for open-angle glaucoma failing topical therapy: 1-year results of a multicenter study. *Am J Ophthalmol*. 2015;159:1075–1081, e1071.
9. Wellik SR, Dale EA. A review of the iStent® trabecular microbypass stent: safety and efficacy. *Clin Ophthalmol*. 2015;9:677–684.
10. Patrianakos TD. Anatomic and physiologic rationale to be applied in accessing the suprachoroidal space for management of glaucoma. *J Cataract Refract Surg*. 2014;40:1285–1290.
11. Hoh H, Grisanti S, Grisanti S, Rau M, Ianchulev S. Two-year clinical experience with the CyPass micro-stent: safety and surgical outcomes of a novel supraciliary micro-stent. *Klin Monbl Augenheilkd*. 2014;231:377–381.
12. Ayton LN, Blamey PJ, Guymer RH, et al. First-in-human trial of a novel suprachoroidal retinal prosthesis. *PLoS One*. 2014;9:e115239.
13. Olsen TW, Feng X, Wabner K, Csaky K, Pambuccian S, Cameron JD. Pharmacokinetics of pars plana intravitreal injections versus microcannula suprachoroidal injections of bevacizumab in a porcine model. *Invest Ophthalmol Vis Sci*. 2011;52:4749–4756.
14. Abarca EM, Salmon JH, Gilger BC. Effect of choroidal perfusion on ocular tissue distribution after intravitreal or suprachoroidal injection in an arterially perfused ex vivo pig eye model. *J Ocul Pharmacol Ther*. 2013;29:715–722.
15. Tyagi P, Barros M, Stansbury JW, Kompella UB. Light-activated, in situ forming gel for sustained suprachoroidal delivery of bevacizumab. *Mol Pharm*. 2013;10:2858–2867.
16. Touchard E, Berdugo M, Bigey P, et al. Suprachoroidal electrotransfer: a nonviral gene delivery method to transfect the choroid and the retina without detaching the retina. *Mol Ther*. 2012;20:1559–1570.
17. Peden MC, Min J, Meyers C, et al. Ab-externo AAV-mediated gene delivery to the suprachoroidal space using a 250 micron flexible microcatheter. *PLoS One*. 2011;6:e17140.
18. Tzameret A, Sher I, Belkin M, et al. Transplantation of human bone marrow mesenchymal stem cells as a thin subretinal layer ameliorates retinal degeneration in a rat model of retinal dystrophy. *Exp Eye Res*. 2014;118:135–144.
19. Kim YC, Oh KH, Edelhauser HF, Prausnitz MR. Formulation to target delivery to the ciliary body and choroid via the suprachoroidal space of the eye using microneedles. *Eur J Pharm Biopharm*. 2015;95:398–406.
20. Gu B, Liu J, Li X, Ma Q, Shen M, Cheng L. Real-time monitoring of suprachoroidal space (SCS) following SCS injection using ultra-high resolution optical coherence tomography in guinea pig eyes. *Invest Ophthalmol Vis Sci*. 2015;56:3623–3634.
21. Kim YC, Edelhauser HF, Prausnitz MR. Particle-stabilized emulsion droplets for gravity-mediated targeting in the posterior segment of the eye. *Adv Healthc Mater*. 2014;3:1272–1282.
22. Chiang B, Kim YC, Edelhauser HF, Prausnitz MR. Circumferential flow of particles in the suprachoroidal space is impeded by the posterior ciliary arteries. *Exp Eye Res*. 2016;145:424–431.
23. Wang M, Liu W, Lu Q, et al. Pharmacokinetic comparison of ketorolac after intracameral, intravitreal, and suprachoroidal administration in rabbits. *Retina*. 2012;32:2158–2164.
24. Seiler GS, Salmon JH, Mantuo R, Feingold S, Dayton PA, Gilger BC. Effect and distribution of contrast medium after injection into the anterior suprachoroidal space in ex vivo eyes. *Invest Ophthalmol Vis Sci*. 2011;52:5730–5736.
25. Kadam RS, Williams J, Tyagi P, Edelhauser HF, Kompella UB. Suprachoroidal delivery in a rabbit ex vivo eye model: influence of drug properties, regional differences in delivery, and comparison with intravitreal and intracameral routes. *Mol Vis*. 2013;19:1198–1210.
26. Moses RA. Detachment of ciliary body–anatomical and physical considerations. *Invest Ophthalmol*. 1965;4:935–941.
27. Tasman W, Jaeger E. *Duane's Ophthalmology*. 15th ed. Philadelphia: Lippincott Williams & Wilkins; 2009.
28. Benchabane A, Bekkour K. Rheological properties of carboxymethyl cellulose (CMC) solutions. *Colloid Polym Sci*. 2008;286:1173–1180.

29. Chiang B, Kim YC, Edelhauser HF, Prausnitz MR. Circumferential flow of particles in the suprachoroidal space is impeded by the posterior ciliary arteries. *Exp Eye Res*. 2016;145:424–431.
30. Chiang B, Wang K, Ethier CR, Prausnitz MR. Clearance kinetics and clearance routes of molecules from the suprachoroidal space after microneedle injection. *Invest Ophthalmol Vis Sci*. 2017;58:545–554.
31. BarbosaSaliba J, Vieira L, Fernandes-Cunha GM, et al. Anti-inflammatory effect of dexamethasone controlled released from anterior suprachoroidal polyurethane implants on endotoxin-induced uveitis in rats. *Invest Ophthalmol Vis Sci*. 2016;57:1671–1679.
32. Danylkova N, Gupta N, Jhaveri CD, Gill MK. Suprachoroidal silicone oil migration following retinal detachment repair. *Ophthalmic Surg Lasers Imaging Retina*. 2013;44:284–286.
33. Wang XH, Li S, Liang L, Xu XD, Zhang XZ, Jiang FG. Evaluation of RGD peptide hydrogel in the posterior segment of the rabbit eye. *J Biomater Sci Polym Ed*. 2013;24:1185–1197.
34. Gilger BC, Wilkie DA, Clode AB, et al. Long-term outcome after implantation of a suprachoroidal cyclosporine drug delivery device in horses with recurrent uveitis. *Vet Ophthalmol*. 2010;13:294–300.
35. Gilger BC, Salmon JH, Wilkie DA, et al. A novel bioerodible deep scleral lamellar cyclosporine implant for uveitis. *Invest Ophthalmol Vis Sci*. 2006;47:2596–2605.
36. Krohn J, Bertelsen T. Corrosion casts of the suprachoroidal space and uveoscleral drainage routes in the human eye. *Acta Ophthalmol Scand*. 1997;75:32–35.
37. Chiang B, Venugopal N, Edelhauser HF, Prausnitz MR. Distribution of particles, small molecules and polymeric formulation excipients in the suprachoroidal space after microneedle injection. *Exp Eye Res*. 2016;153:101–109.
38. Ugarte M, Hussain AA, Marshall J. An experimental study of the elastic properties of the human Bruch's membrane-choroid complex: relevance to ageing. *Br J Ophthalmol*. 2006;90:621–626.
39. Daxer A, Misof K, Grabner B, Ettl A, Fratzl P. Collagen fibrils in the human corneal stroma: structure and aging. *Invest Ophthalmol Vis Sci*. 1998;39:644–648.
40. Ethier CR, Johnson M, Ruberti J. Ocular biomechanics and biotransport. *Annu Rev Biomed Eng*. 2004;6:249–273.
41. Emi K, Pederson JE, Toris CB. Hydrostatic pressure of the suprachoroidal space. *Invest Ophthalmol Vis Sci*. 1989;30:233–238.
42. Kim YC, Edelhauser HF, Prausnitz MR. Targeted delivery of antiglaucoma drugs to the supraciliary space using microneedles. *Invest Ophthalmol Vis Sci*. 2014;55:7387–7397.
43. Chiang B, Kim YC, Doty AC, Grossniklaus HE, Schwendeman SP, Prausnitz MR. Sustained reduction of intraocular pressure by supraciliary delivery of brimonidine-loaded poly(lactic acid) microspheres for the treatment of glaucoma. *J Control Release*. 2016;228:48–57.
44. El Rayes EN, Oshima Y. Suprachoroidal buckling for retinal detachment. *Retina*. 2013;33:1073–1075.
45. Poole TA, Sudarsky RD. Suprachoroidal implantation for the treatment of retinal detachment. *Ophthalmology*. 1986;93:1408–1412.

Investigative Ophthalmology & Visual Science